Available online at www.sciencedirect.com
SCIENCE DIRECT®
PERGAMON
International Journal of Heat and Mass Transfer 46 (2003) 3755–3764
International Journal of HEAT and MASS TRANSFER
www.elsevier.com/locate/ijhmt

Effusivity-based correlation of surface property effects in pool boiling CHF of dielectric liquids

Mehmet Arik [a], Avram Bar-Cohen [b,*]

[a] General Electric Company, Global Research Center, Energy and Propulsion Technologies, Thermal Systems Laboratory, One Research Circle ES-102, Niskayuna, NY 12309, USA

[b] Laboratory for Thermal Packaging of Electronic Systems, Department of Mechanical Engineering, University of Maryland, College Park, MD 20742, USA

Received 6 May 2002; received in revised form 11 April 2003

Abstract

Although the effects of fluid properties, pressure, and subcooling, as well as heater geometry, on the pool boiling critical heat flux, or CHF, are relatively well established, explanations for the surface property effects remain controversial. Proposed formulations, embodying the dependence of CHF on the product of the heater thermal effusivity and thickness are described and compared with available data. A composite correlation for pool boiling CHF, accounting for the conduction and hydrodynamic limits, as well as the effects of pressure, subcooling, and length, is proposed. This effusivity-based correlation is found to predict a broad range of pool boiling CHF data for dielectric liquids, for thermal effusivity values between 0.2 and 120, pressure from 100 to 450 kPa, and subcoolings from 0 to 75 K, with a standard deviation of 12.5%.

1. Introduction

Despite the precipitous drop in transistor switching energy that has characterized the solid-state semiconductor revolution, the cooling requirements of microelectronic components have not diminished. As the 21st century begins, high performance chip power dissipation exceeds 100 W, some three orders-of-magnitude above the chips of the early 1960s, and informed opinion suggests that power dissipation will continue rise over the rest of the present decade [1]. Thermal management is thus one of the key challenges in advanced electronic packaging and considerable improvement in thermal packaging will be needed to successfully exploit the "Moore's Law" acceleration in semiconductor technology.

In the late 1990s, under the influence of market forces, thermal management of nearly all the products in the "High Performance" category devolved to the aggressive use of air cooling, exploiting technology that was a natural outgrowth of the air-cooled multichip modules of the 1980s. Thus, by the end of the decade, a renaissance in thermal packaging produced heat sinks for high-end commercial workstations and servers that were routinely dissipating 60–70 W, with chip heat fluxes of some 26 $W\,cm^{-2}$. The packaging community consensus suggests that early in the second decade of this century power dissipation will rise to 175 W for chips operating at some 3 GHz. It is anticipated that chip area, growing from 3.8 cm^2 to some 7.5 cm^2, will keep pace with chip power dissipation in the coming years, yielding average chip heat fluxes that increase only marginally above the present values to approximately 30 $W\,cm^{-2}$ by 2006, before beginning a slow decline in later years. However, growing use of system-on-a-chip concepts, is producing large variations in heat flux, with peak values expected to exceed 100 $W\,cm^{-2}$ [1,2].

Cost-effective thermal management of large silicon chips with power dissipation approaching 200 W requires exploration of non-conventional thermal packaging techniques, including direct cooling with dielectric

* Corresponding author. Tel.: +1-301-405-3173; fax: +1-301-314-9477.
E-mail address: barcohen@eng.umd.edu (A. Bar-Cohen).

0017-9310/03/$ - see front matter © 2003 Elsevier Ltd. All rights reserved.
doi:10.1016/S0017-9310(03)00215-1

Nomenclature

c_p	specific heat [J kg^{-1} K^{-1}]
CHF	critical heat flux [W m^{-2}]
g	gravitational acceleration [m s^{-2}]
h	heat transfer coefficient [W m^{-2} K^{-1}]
h_{fv}	latent heat of evaporation [J kg^{-1}]
Ja	Jacob number
k	thermal conductivity [W m^{-1} K^{-1}]
L	length of the heater [m]
L'	non-dimensional characteristic length $[L(g(\rho_f - \rho_v)/\sigma)^{1/2}]$
r	radial coordinate [m]
R	radius of the heater [m]
S	thermal activity parameter $[\delta(\rho c_p k)^{1/2}]$
q''	heat flux [W m^{-2}]
t	time [s]
T	temperature [°C]
z	axial coordinate [m]

Greek symbols

α	proportional
δ	thickness [m]
λ_D	Taylor wavelength [m]
ρ	density [kg m^{-3}]
σ	surface tension [N m^{-1}]
τ_D	hovering period [s]
ΔT	temperature difference [K]

Subscripts

boil	boiling
d	dry spot
ex	experimental
f	liquid
gen	generation
h	heater
ini	initial
m	measured
pre	predicted
rad	radial
sat	saturation
sub	subcooling
sur	surface
TME	thermal management of electronics
v	vapor

liquids [3]. The high dielectric strength and low dielectric constant of these liquids, as well as their chemical inertness, make it possible to immerse most electronic components directly in these fluorochemical liquids. Pool boiling on the chip surface transfers the dissipated heat directly into the liquid and, thus, overcomes the barrier posed by the interface resistance otherwise encountered at the solid interface between the chip and the cooling hardware. With saturated pool boiling, component heat fluxes in the range of 10–20 W cm^{-2} could be removed at surface superheats of typically less than 20 K.

The critical heat flux (i.e. CHF), places an upper limit on this highly efficient heat transfer process. Heat fluxes in excess of CHF result in the formation of an insulating film of vapor on the heat transfer surface and superheats typically higher by an order-of-magnitude than encountered in nucleate pool boiling. Most predictive models for pool boiling CHF are based on the analysis of hydrodynamic phenomena leading to the "choking off", or interruption, of the liquid supply to the heater [4]. These models fail to account for the effect on CHF of heater thermophysical properties. Yet, it has been widely known that the thermal properties of the heated surface, such as thickness, thermal conductivity, and specific heat, affect the pool boiling CHF and that the CHF increases asymptotically with various combinations of these properties [5]. However, much of the existing data pertains to conventional heat exchanger tube and plate materials and is thus not relevant to electronic cooling applications. A better understanding of the effect of thermal properties and thickness on the CHF is necessary if pool boiling of dielectric liquids is to serve as a viable technique for the thermal management of electronic components.

2. Prior literature

2.1. CHF theory

Noting the similarity between pool boiling CHF and "flooding" in distillation columns, Kutateladze [6] obtained an expression for CHF based on a similitude analysis of the momentum and energy equations for two-phase flow near the heated surface. Subsequently, Zuber [7] derived an analytical equation for CHF controlled by the hydrodynamic instability of rising columns of vapor. Assuming that CHF occurred when the interface between the liquid and vapor streams became unstable, and completely choked off the flow to the surface, he proposed the following:

$$q''_{CHF} = \frac{\pi}{24} h_{fv} \sqrt{\rho_v} [\sigma_f g(\rho_f - \rho_v)]^{1/4} \quad (1)$$

This correlation was calibrated specifically to saturated pool boiling on large, thick, upward-facing horizontal plates and provides a convenient and well-recognized baseline correlation for pool boiling CHF [4].

Photographic studies by Gaertner and Westwater [8] and Gaertner [9] failed to demonstrate the presence of unstable vapor columns on large horizontal flat plates and, in the more recent experiments by Williamson and El-Genk [10], evidence was found for lateral bubble coalescence leading to the formation of large mushrooms on the heater surface.

The periodic formation and departure of such vapor mushrooms is at the heart of the macrolayer model, proposed earlier by Haramura and Katto [11], which postulates that CHF is associated with complete vaporization of the "macrolayer" of liquid trapped beneath this vapor mushroom. However, visual observations of pool boiling by Kirby and Westwater [12], and Van Querkerk [13] have shown that dry patches on the heater can be re-wet by the liquid after the departure of the vapor mushroom.

Thus, macrolayer evaporation and local surface dryout are not sufficient to cause CHF. Rather, following Ramilson and Lienhard [14], for CHF to occur, it appears necessary for the temperature of the dry patch to reach the Leidenfrost point beyond which liquid–solid contact is no longer possible [4]. The Unal et al. [15] conduction-centered numerical investigation of saturated pool boiling supported this "hot spot" controlled CHF mechanism.

2.2. Thermal properties—experimental results

Bernath [16] was, perhaps, the first researcher to investigate the effects of thermal properties and thickness of the heater on the CHF by observing that thicker heaters produced higher CHF than thinner structures. His research on vertically oriented cylindrical heaters in water was later extended to both solid and hollow cylinders. Experimental results revealed that the solid cylinders had about 43% higher CHF than hollow structures [16].

A study employing zirconium ribbon heaters immersed in toluene, was performed by Cole and Shulman [17]. Experimental results were similar to previously published studies, with 42% higher CHF for the thickest heater. Generally similar results were found by Carne and Charlesworth [18], who completed a detailed set of experiments, with a wider heater thickness selection, using ribbon heaters in saturated *n*-propanol, Tachibana et al. [19], who performed a series of experiments with a variety of materials and thickness in water, Guglielmini and Nanei [20], whose experimental study involved the use of different cylindrical heaters formed with an electroplating technique, Grigoriev et al. [21], whose experimental study with circular copper heaters in helium showed that CHF increased asymptotically until a thickness of 350 μm, and Bar-Cohen and McNeil [5], who showed that the CHF on thin, sputtered horizontal platinum heaters was inferior to relatively thick, doped silicon heaters boiling in dielectric liquids.

Caravalho and Bergles [22] performed an extensive study on the thermal property effect. Their experimental study showed that thick copper blocks experienced higher CHF. But the Zuber [7] relationship was found to over predict CHF by as much as 50%.

A comprehensive experimental study to determine the effects of thermal conductance/capacitance of the heater on CHF was performed by Golobic and Bergles [23]. Using heaters fabricated of 10 different materials in a wide range of thicknesses (from 2 to 1000 μm), they determined the saturated FC-72 pool boiling CHF on horizontally suspended, vertically oriented, ribbon heaters. Fifty data sets for 5 mm high by 50 mm wide ribbons were reported. The asymptotic CHF value for the heaters was found to equal 13.5 $\mathrm{W\,cm^{-2}}$. The empirical CHF values were non-dimensionalized by the asymptotic CHF values and correlated.

Chang and You [24] performed experiments with heaters of various thicknesses, boiling in saturated FC-72 under atmospheric pressure with a non-dimensional heater characteristic length, L', of 13.8. The thinnest heaters were created by sputtering thin platinum films on a glass substrate. Thick heater experiments were performed with copper heaters at various thicknesses.

The ratio of the experimental results to the classical Zuber prediction displayed the asymptotic behavior of CHF. A summary of these studies is given in Table 1.

2.3. Effusivity based proposed correlations

The first documented attempt to correlate heater surface property effects on pool boiling CHF was reported by Carne and Charlesworth [18]. Based on their experimental results with *n*-propanol, they proposed that the effect of the heater could be best correlated with the product of thickness and thermal conductivity. This correlating parameter was derived from the assertion that some regions of the heater had more nucleation sites resulting in higher local heat flux values.

Tachibana et al. [19] related the surface property effect to transient conduction in areas of the heater surface shrouded by vapor, preventing fresh liquid from wetting the surface and leading to CHF. This effect, they believed, could be correlated with the product of the volumetric heat capacity and the thickness.

Guglielmini and Nanei's [20] observation that thin cylindrical heaters experienced lower CHF led them to a correlation of the thickness required to achieve 90% of the "symptotic" CHF. This thickness, δ_{90}, was found to vary inversely with the thermal effusivity to the 3.26 power, as

$$\delta_{90} = C\left(\sqrt{\rho_{\mathrm{h}} c_{\mathrm{p_h}} k_{\mathrm{h}}}\right)^{-3.26} \tag{2}$$

Table 1
Summary of the heater geometry and thermal properties of the CHF studies

Author(s)	Liquid	Material	$L' = (L * \Delta\rho/\sigma)$	$S = (\rho c_p k)^{0.5}$
You [28]	FC-72	Pt	$6.9 < L' < 13.8$	0.26
Chang and You [24]	FC-72	Cu	13.8	$21.5 < S < 119$
Arik [27]	FC-72, Novec fluids	Si, BeO	$4.9 < L' < 13.8$	$1.6 < S < 15.7$
Watwe and Bar-Cohen [26]	FC-72	Si	13.8	4.7
Mudawar et al. [31]	FC72	Cu	$15 < L' < 150$	29.7
Golobic and Bergles [23]	FC-72	Al, Cu, etc.	6.9	$S < 8$

A comprehensive review of the experimental results and proposed correlations of the heater property effects on CHF, led Saylor [25] to propose a hybrid "thermal activity" parameter, S, equal to the product of the heater thickness and the thermal effusivity, as

$$S = \delta\sqrt{\rho_h c_h k_h} \tag{3}$$

Bar-Cohen and McNeil [5] found the effect of S on the CHF data, for sputtered horizontal platinum heaters and doped silicon heaters in dielectric liquids (providing a range of S values from 0.1 to 25), could be correlated in the form:

$$\frac{q_{CHF}}{q_{CHF,asy}} \propto \frac{S}{S+0.8} \tag{4}$$

where S is the thermal activity parameter defined in Eq. (3). This relationship yields 90% of the asymptotic CHF value for S equal to 8, while the 1% approach (99% of the asymptotic CHF) is attained at $S = 85$.

A more extensive literature review, focusing on low S value heaters, and including supporting numerical studies on the transient temperature rise of relatively thin heaters with poor thermal properties, led Watwe and Bar-Cohen [26] to embrace the product of the thermal effusivity, with the heater thickness in the correlation of CHF. In detailed numerical simulations, the temperature rise of a point in the center of a region blanketed by vapor was found to be controlled by radial diffusion, and to be governed by a relation of the form [26]:

$$T_{sur} - T_{ini} = f\left(\frac{qR_d}{\delta\sqrt{\rho_h c_{p_h} k_h}}, \frac{r}{R}, \sqrt{t}\right) \tag{5}$$

Following closely on the proposals of Ramilson and Lienhard [14] and Unal et al. [15], the Watwe-Bar-Cohen [26] model is predicated on the assumption of an ever present non-uniform nucleation site density on the heater surface, which results in the formation of local vapor mushrooms, via lateral coalescence of individual vapor bubbles or the collapse of vapor columns. The depletion of the liquid under these vapor mushroom then leads to the creation of local dry spots, whose temperature rises steeply under the influence of the imposed heat flux. This temperature rise rate is moderated by the ability of the underlying structure to locally absorb and/or conduct heat to parts of the heater still experiencing nucleate boiling (see Fig. 1).

If the temperature of the dry patch, at the end of the residence (or "hovering") time of the vapor mushroom, exceeds the Leidenfrost temperature, the returning liquid is unable to quench the overheated surface, local dry out proceeds to global dry out, and CHF is said to occur. If the heater is very thin and has poor thermal properties, the dry patch temperature may exceed the Leidenfrost critical temperature soon after the formation of the first dry spot anywhere on the heater surface. CHF on such heaters will then be highly sensitive to the non-uniformities in the nucleation site density and dependent on the S value of the surface, yielding a diffusion-driven lower limit on CHF. At the other end of the spectrum, the heater thickness and thermal properties may be so large as to successfully absorb and conduct the heat away from the local dry patch for an extended period, thus keeping the dry patch temperature from exceeding the critical re-wet temperature. For such a high-S situation, the heater may be able to sustain the sequential formation and extinction of many dry spots, relying on the subsequent re-wetting of the surface to locally cool the surface back to the nucleate boiling regime. CHF on such heaters would, then, occur primarily due to a hydrodynamic instability resulting in an extensive interruption of liquid flow to the heater. The hydrodynamic instability models would,

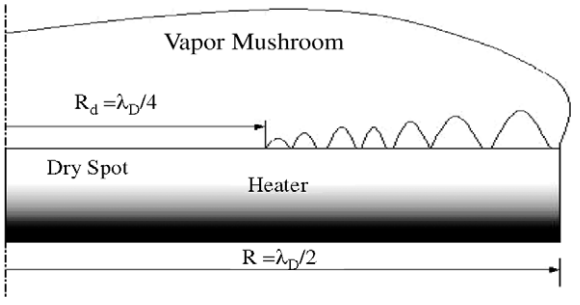

Fig. 1. Axis-symmetric model for the numerical analysis [26].

therefore, provide the upper or asymptotic limit for CHF.

The TME Laboratory correlation for pool boiling CHF, which was derived for horizontal, square heaters and is presented in Fig. 2 [26], is shown in Eq. (6) to take the form;

$$q''_{\mathrm{CHF,TME}} = \frac{\pi}{24} h_{\mathrm{fv}} \sqrt{\rho_{\mathrm{v}}} [\sigma_{\mathrm{f}} g(\rho_{\mathrm{f}} - \rho_{\mathrm{v}})]^{1/4} \left(\frac{S}{S+0.1} \right) \times [1 + \langle 0.3014 - 0.01507 L'(P) \rangle] \times \left(1 + 0.030 \left[\left(\frac{\rho_{\mathrm{f}}}{\rho_{\mathrm{v}}} \right)^{0.75} \frac{c_{\mathrm{Pf}}}{h_{\mathrm{fv}}} \right] \Delta T_{\mathrm{sub}} \right) \quad (6)$$

where

$$L'(P) = L \sqrt{\frac{g(\rho_{\mathrm{f}} - \rho_{\mathrm{v}})}{\sigma}}$$

The first term on the right side represents the classical Kutateladze–Zuber prediction, considered the upper limit, saturation value of CHF on very large horizontal heaters [7]. The second term is the effect of heater thickness and thermal properties. The third term accounts for the influence of the length scale on the CHF and is equal to unity or higher. The last term represents the influence of subcooling on CHF. Examination of Eq. (6) reveals that the approach of CHF to the asymptotic limit takes the form;

$$\frac{q_{\mathrm{CHF}}}{q_{\mathrm{CHF,asy}}} \propto \frac{S}{S+0.1} \quad (7)$$

The CHF values calculated via Eq. (7) reach 90% of the asymptotic CHF value when S is equal to 1, while the 1% approach occurs at $S = 10$. It should, however, be noted that the S range in their data was relatively modest, spanning values from 0.5 to 4.7.

Golobic and Bergles [23] offer an alternative correlation of the heater surface effects on CHF, based on their experimental study of saturated pool boiling CHF in FC-72. These authors also correlated the influence of the heater material on CHF in terms of the S parameter, defined in equation (3). However, their relation took the form [23],

$$\frac{q_{\mathrm{CHF}}}{q_{\mathrm{CHF,asy}}} = 1 - \mathrm{e}^{-[S/2.44]^{0.8498} - [S/2.44]^{0.0581}} \quad (8)$$

Thus, the three most recent correlations of the heater surface effects on CHF [5,23,26], all embody the dependence of CHF on the product of the heater thermal effusivity and thickness. Plotting these relation in Fig. 3, is to be noted that all three relations (Eqs. (4), (7) and (8)) yields nearly identical CHF values for S greater than 50, and all reach 90% of the asymptotic CHF value when S is higher than 8. However, significant differences do exist at intermediate values of S. Examining Fig. 3, it may be seen that the locus of Eq. (8) lies between the loci of Eqs. (5) and (7), while, at very low S values, the Golobic and Bergles relation (Eq. (8)) yields higher fractions of the asymptotic CHF than the other correlations, e.g. when S equals 0.001, use of Eq. (8) results in $q_{\mathrm{CHF}}/q_{\mathrm{asy}}$ of 0.521 vs. 0.0123 for Eq. (5).

3. Pool boiling CHF experimental investigation

3.1. Experimental apparatus

The present study was aimed at expanding the range of available S data and included additional experiments on the heater surface effect on pool boiling CHF, in the presence of subcooling and elevated

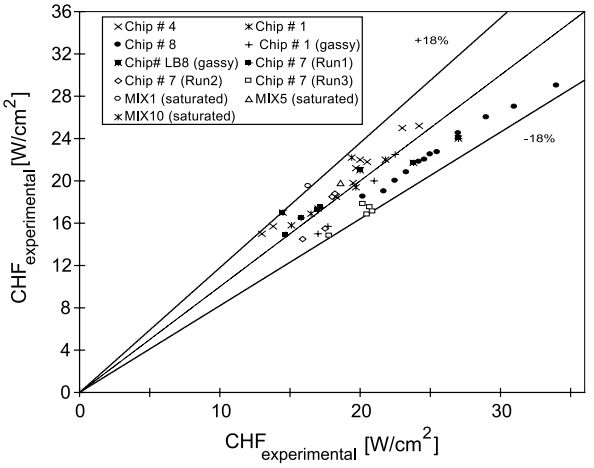

Fig. 2. Experimental and predicted pool boiling CHF values with PPGA chips [27].

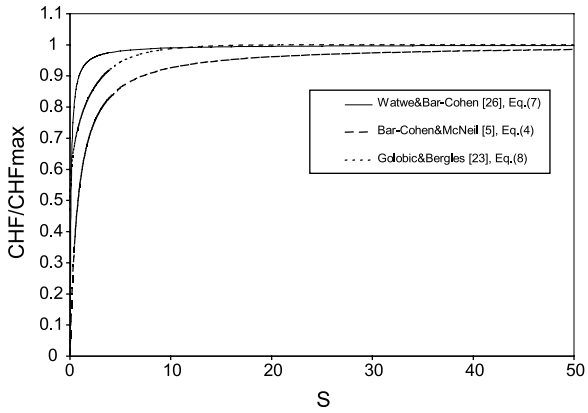

Fig. 3. Variation of dimensionless pool boiling CHF with thermal activity parameter.

pressure, for the parametric range shown in Table 1. Fig. 4 shows the test set-up for the CHF experiments, originally designed by You [28], and modified for the current study. Experiments were conducted in a stainless steel test vessel operated up to 500 kPa in pressure. The tank includes two windows for the visual observation of the heat transfer phenomenon from the chip package.

A lexan container filled with water is used to control the coolant temperature in the vessel. To condition the test fluid (FC-72 or Novec fluids), coolant is passed through a copper coil, which is immersed in the water. A magnetic stirring system is placed in the test vessel to create a homogenous temperature distribution in the vessel.

A dual type pressure gauge is connected to the flow loop to observe the pressure visually. In addition, a piezo-resistive pressure transducer is placed on the cover of the test vessel to measure the pressure in the tank. A precision resister is used to accurately measure the current flowing in the power line. Temperature measurements were performed with diodes and thermocouples. The fluid, FC-72, temperature was measured by using five T-type thermocouples. Further details of this apparatus may be found in [27].

3.2. Test packages

Although several different test packages were used in this study, the majority of the tests was performed with the ATC2.6 chip packages, shown in Figs. 5 and 6, and obtained from Sandia National Laboratories [29]. These dual-in-line chip packages, or DIPs, have 40 pins for the

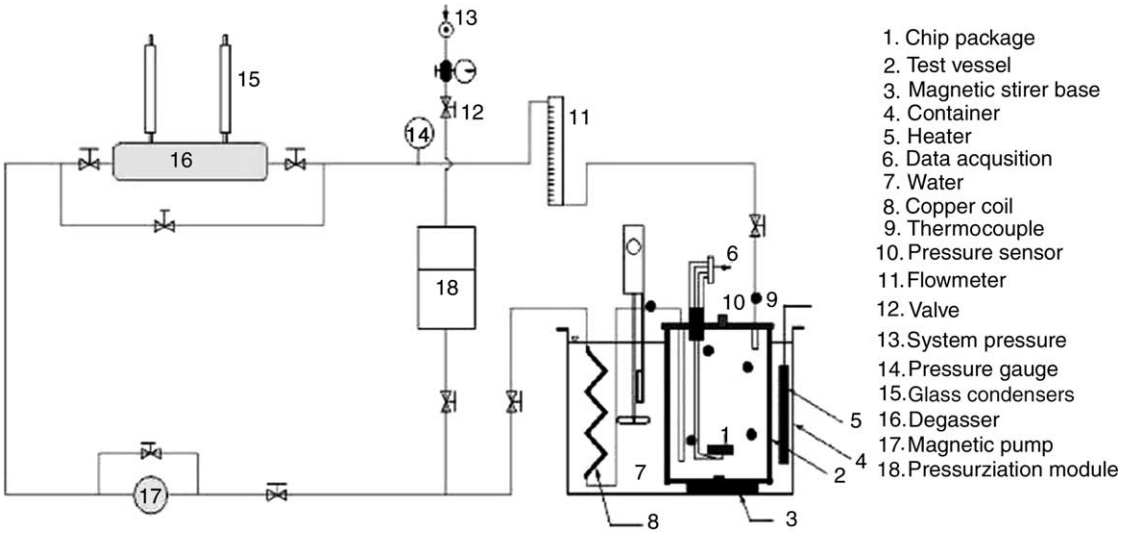

Fig. 4. Pool boiling experimental set-up.

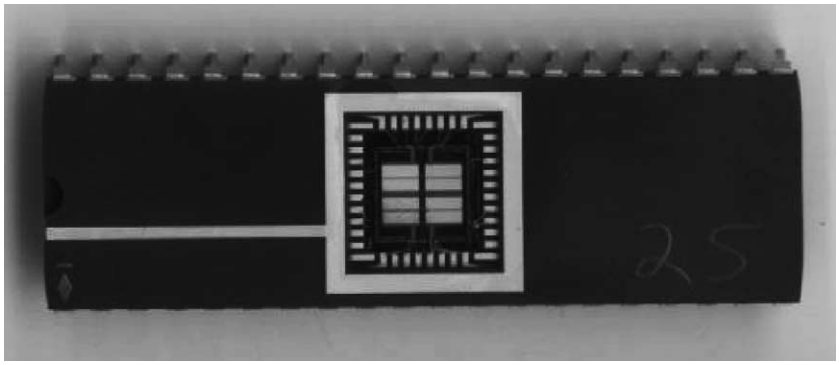

Fig. 5. Dual-in-line package, DIP by Sandia National Labs.

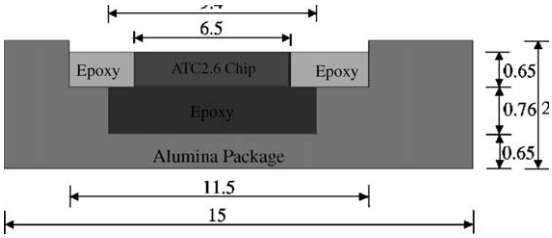

Fig. 6. Schematic diagram of the ATC2.6 chip packages.

electrical connections and measurements. A silicon die (6.4×6.4 mm) was embedded in a cavity and attached to the package by means of a low conductivity epoxy. The chip carries two heater structures on 2 μm lines and spacings using polysilicon conductors oriented perpendicularly to the overlying triple tracks with a nominal resistance of 50 ohms. This package provides five p^+n diode thermometers, one in the die center and four under the perimeter bondpads. Three distinct ATC2.6 packages, containing silicon chips of 100, 300, and 625 μm in thicknesses and providing S values of 1.56, 4.7, and 9.8 ($J\,mKs^{-0.5}$), respectively, were tested in the experimental investigation. More detailed information is presented in [27].

3.3. Experimental procedure

The data acquisition system consisted of a Personal Computer working in the UNIX environment, a digital multimeter with a 20-channel factory built, scanner card. Power to the chip was supplied by a programmable DC power supply. A computer program, which worked in the UNIX environment, had been written to control the experiment and get the necessary readings from the system. The computer program controlled the power level, power increments, and readings. Before starting each experimental run, all of the devices were turned on to avoid transient effects. After the required test conditions were assured, the computer program was started. The computer program established the chip power setting and continuously read the diode temperatures to avoid a destructive termination of the experiment, i.e. ''burn-out''. At the end of the waiting period, when the steady state condition for each power level was attained, the final set of readings from diodes, thermocouples and pressure transducers was recorded in a file. Step sizes were varied between 0.2 and 1 W depending on the conditions. When a temperature jump of 30 K occurred, the computer program disabled the power supply. The experimental value of CHF was determined by averaging the last two heat fluxes, prior to the rapid rise in chip temperature.

3.4. Measurement uncertainty

Standard techniques were followed to obtain the experimental uncertainty [30]. The basic uncertainty sources were measurement resolution, substrate heat loses, and calibration errors. Precision errors from readings were decreased by increasing the sample population. The uncertainty in the wall superheat depends on both the surface and the saturation temperature. The overall uncertainty in the wall superheat was estimated to be ~1.5 K. The uncertainty in the actual heat flux from the chip was caused by variation in the voltage readings by the sensor and the current calculation through the precision resistor voltage readings. The maximum uncertainty in the heat flux was found to be $0.66\ W\,cm^{-2}$ within the 95% confidence level, at or near CHF. However, as a result of lower heat transfer coefficients from the package to the liquid during natural convection, the uncertainty in this part of boiling curve, when heat fluxes are more moderate, is $\pm 1.8\ W\,cm^{-2}$. The dual type pressure gauge in the FC-72 flow loop had a bias error of about 0.8%. The uncertainty associated with the pressure transducer installed on the cover of the test vessel is given by the manufacturer as 0.85 kPa.

4. Experimental results

4.1. Isolated surface property effects

The results of the present experiments, with the ATC2.6 packages containing chips of three different thickness, are shown in Fig. 7, where it may be seen that at all pressures and subcoolings tested packages with the largest values of S consistently yielded the highest value of CHF. Fig. 8 presents the experimental findings of Chang and You [24] over a far broader range of S values, revealing the expected effect of copper block thickness on the CHF.

The present data, along with that of Golobic and Bergles [23] and that of Chang and You [24], as well as earlier data discussed above, are plotted in Figs. 9 and 10, in two different scales. To directly observe the functional form of the S dependence, the data are presented in terms of the non-dimensionalized CHF and compared with the three previously discussed effusivity-based relations. Published experimental CHF data were normalized by dividing by the maximum CHF value presented in each study.

It is to be noted that the Golobic and Bergles data has been plotted in two forms—one set non-dimensionalized by their reported empirical CHF asymptote and the other by a length-scale-corrected asymptote. The latter is meant to recognize the contribution of the small ribbon height to CHF, yielding a length scale enhancement of the CHF, which might have masked the strength of the CHF suppression effect produced by the low S values. Interestingly it may be observed in Fig. 9 that the length-scale-corrected Golobic and Bergles data is in better agreement with the other data sets appearing in this comparison.

A careful examination of Fig. 9 reveals that, in the range of $0 < S < 1$, Eqs. (4) and (7) have relative errors (i.e. $\mathrm{abs}(\mathrm{CHF}_{ex} - \mathrm{CHF}_{pre})/\mathrm{CHF}_{ex}$) of 52% and 13%

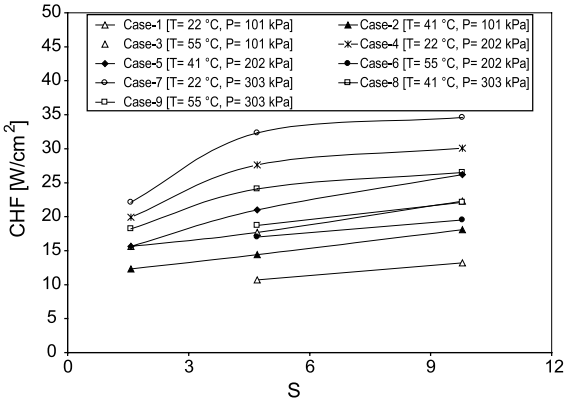

Fig. 7. Variation of pool boiling CHF with thermal activity parameter at various pressures for ATC2.6 chips packages.

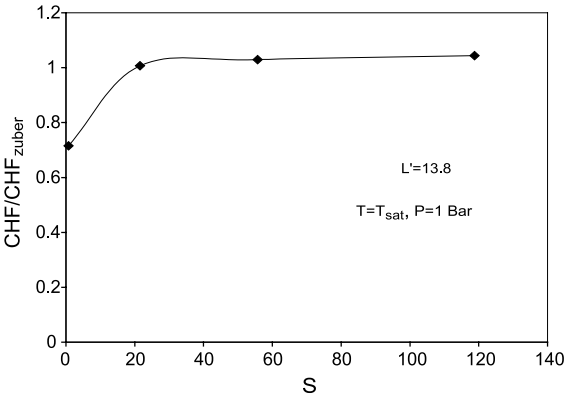

Fig. 8. Effect of thermal activity parameter on the pool boiling CHF at the saturation temperature for copper blocks [24].

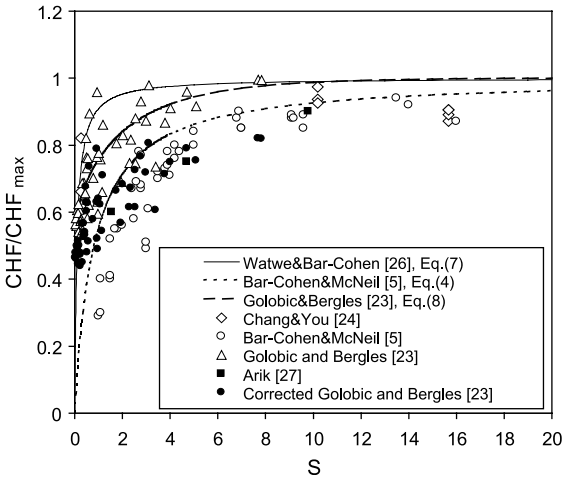

Fig. 9. Variation of the non-dimensional experimental pool boiling CHF values with thermal activity parameter.

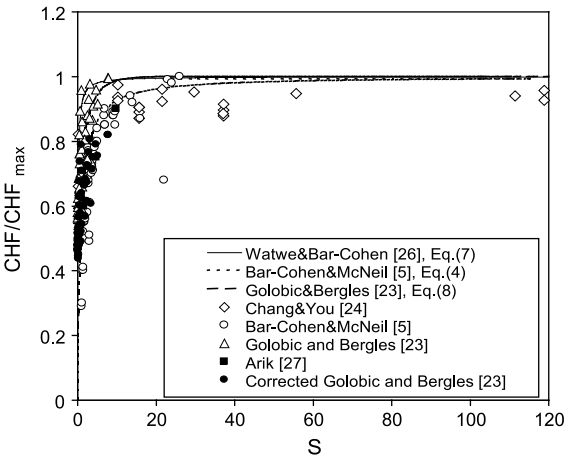

Fig. 10. Variation of the non-dimensional experimental pool boiling CHF values with thermal activity parameter.

respectively, while Eq. (8) is able to predict the experimental non-dimensional CHF values with a 9.2% relative error. When a range between 1 and 10 is considered, these errors become 16%, 21%, and 26% respectively. Finally, if the full range between 0 and 120 is taken into consideration, the Watwe and Bar-Cohen relation [26] predicts the heater effusivity effect with a 16.6% error, while Eqs. (4) and (7) depart from the data by 24% and 18% errors, respectively.

4.2. Effusivity-enhanced CHF correlation

Fig. 11 shows a comparison between the TME correlation and 336 data points, combining data used in the development of the TME correlation with recent published data in the literature. Following [30], the standard deviation between these data points and the correlation were found to be 12.5%. This leads to a 25% uncertainty band with a 95% confidence level in predicting the experimental CHF values. The correlation provides predictions spanning a significant pressure and subcooling range ($0 < P < 4.5$ kPa, $0 < \Delta T_{sub} < 75$ K), various heater materials and geometries ($0.2 < S < 120$), and fluids (dielectric Fluorinert liquids such as FC-72), Novec fluids (i.e. HFE7100 and HFE7200), refrigerants (R113, ethanol, etc.). The effects of heater thickness and the thermophysical properties are successfully addressed through the thermal activity parameter yielding a correlation accuracy similar to that previously reported for thick heaters in which effusivity effects are negligible.

It is to be noted that, due to uncertainties in the thermophysical properties of the relatively new Novec fluids, it appears that prediction of Novec pool boiling CHF displays a larger uncertainty than observed for the other dielectric fluids. These results are, nonetheless included in the present study, since available empirical results have revealed that Novec fluids may be superior to perflourinated liquids [27] and it is anticipated that there use in electronic cooling applications will grow rapidly in the near future.

5. Summary and conclusions

The current effort was devoted to extending the TME pool boiling CHF correlation for horizontal square heaters, embodying an assumed dependence of CHF on the product of the heater thermal effusivity and thickness, to a broad range of between 0.2 and 120. The experimental data is compared to the CHF values predicted by the TME correlation, as well as to other correlation's proposed in the literature. It is found that the TME correlation can predict the pool boiling CHF with a standard deviation of 12.5% for various heater materials and geometries in a large range of subcooling and pressure (0–75 K, 100–450 kPa) conditions within a 95% confidence level.

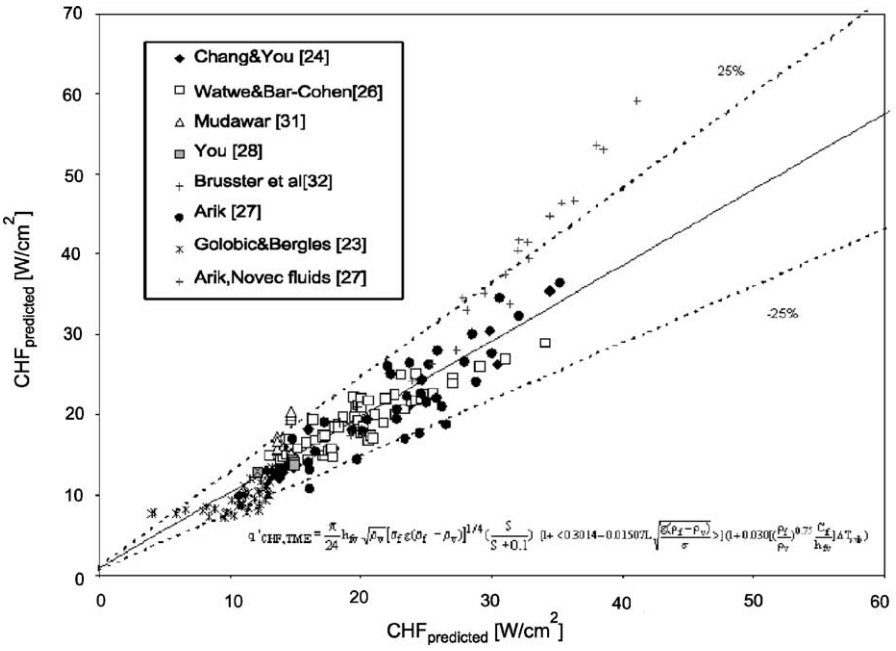

Fig. 11. Experimental and predicted pool boiling CHF values for a broad range of data [23,24,26–28,31,32].

References

[1] SIA, The National Technology Roadmap for Semiconductors: Technology Needs—1997, Semiconductor Industry Association, Washington, DC, 1997.

[2] NEMI, National Electronics Manufacturing Technology Roadmaps, 1996.

[3] A.E. Bergles, A. Bar-Cohen, Direct liquid cooling of microelectronic components, in: Advances in Thermal Modeling of Electronic Components and Systems, vol. 2, ASME Press, New York, 1990, pp. 233–342.

[4] V.P. Carey, Liquid–vapor phase change phenomena: an introduction to the thermophysics of vaporization and condensation processes in heat transfer equipment, February 1992.

[5] A. Bar-Cohen, A. McNeil, Parametric effects on pool boiling critical heat flux in highly wetting liquids, in: Proceedings of Engineering Foundation Conference on Pool and External Flow Boiling, CA, 1992, pp. 171–176.

[6] S.S. Kutateladze, A hydrodynamic theory of changes in the boiling process under free convection conditions, Izv. Akad. Nauk SSSR, Otd. Tekhn. Nauk No. 4 (translation in AEC-TR-1441), 00.529, 1951.

[7] N. Zuber, Atomic energy commission technical information service, Atomic Energy Commission Report AECU-4439, 1959.

[8] R.F. Gaertner, J.W. Westwater, Population of active sites in nucleate boiling heat transfer, Chem. Eng. Prog. Ser. Symp. 56 (1960) 39–48.

[9] R.F. Gaertner, Photographic study of nucleate boiling on a horizontal surface, J. Heat Transfer 87 (1965) 17–29.

[10] C.R. Williamson, M.S. El-Genk, High speed photographic analysis of saturated nucleate pool boiling at low heat flux, ASME Paper 91-WA-HT-8, 1991.

[11] Y. Haramura, Y. Katto, A new hydrodynamic model or CHF applicable widely to both pool and forced convection boiling on submerged bodies in saturated liquids, Int. J. Heat Mass Transfer 26 (1983) 389–399.

[12] D.B. Kirby, J.W. Westwater, Bubble and vapor behavior on a heated horizontal plate during pool boiling near burnout, Chem. Eng. Prog. Ser. 57 (1965) 238–248.

[13] J.H. Van Querkerk, Burnout in pool boiling: the stability of boiling mechanism, Int. J. Heat Mass Transfer 15 (1972) 25–34.

[14] J.M. Ramilson, J.H. Lienhard, Transition boiling heat transfer and film transition regime, J. Heat Transfer 109 (1987) 746–752.

[15] C. Unal, P. Sadasivan, R.A. Nelson, On the hot spot controlled critical heat flux mechanism in pool boiling of saturated fluids, Pool and External Flow Boiling—ASME 1992, 1992, pp. 193–201.

[16] L. Bernath, A theory of local-boiling burnout and its application to existing data, Chem. Eng. Prog. Symp. Ser. 56 (1960) 95.

[17] R. Cole, H.L. Shulman, Critical heat flux at sub-atmospheric pressures, Chem. Eng. Sci. 21 (1966) 723–724.

[18] M. Carne, D.H. Charlesworth, Thermal conduction effects on the CHF in pool boiling, Chem. Eng. Prog. Symp. Ser. 62 (1966) 24.

[19] F. Tachibana, M. Akiyama, H. Kawamura, Non hydrodynamic aspects of pool boiling burnout, J. Nucl. Sci. Technol. 4 (1967) 121.

[20] G. Guglielmini, E. Nannei, On the effect of heating wall thickness on pool boiling burnout, Int. J. Heat Mass Transfer 19 (1976) 1073.

[21] V.A. Grigoriev, V.V. Klimenko, Yu.M. Pavlov, Ye.V. Amitestov, The influence of some heating surface properties on the CHF in cryogenics liquids boiling, in: Proceedings of the 6th International Heat Transfer Conference, vol. 1, 1978, p. 215.

[22] R.D.M. Caravalho, A.E. Bergles, The effects of the heater thermal conductivity/capacitance on the pool boiling CHF, in: Proceedings of the Engineering Foundation Conference on Pool and External Flow Boiling, Santa Barbara, 1992, p. 203.

[23] I. Golobic, A.E. Bergles, Effects of heater side factors on the saturated pool boiling critical heat flux, Exp. Thermal Fluid Sci. 5 (1997) 43–51.

[24] J.Y. Chang, S.M. You, Pool boiling heat transfer from inclined, micro-porous surfaces simulating microelectronics devices, in: Interpack'97, ASME EEP-vol. 19-2, 1997, p. 2055.

[25] J.R. Saylor, An experimental study of the size effect in pool boiling CHF on square surfaces, Master's Thesis, Department of Mechanical Engineering, University of Minnesota, Minneapolis, Minnesota, 1989.

[26] A.A. Watwe, A. Bar-Cohen, Modeling of conduction effects on pool boiling CHF of dielectric liquids, in: Proceedings of National Heat Transfer Conference, 1997, p. 35.

[27] M. Arik, Enhancement of pool boiling critical heat flux in dielectric liquids, Ph.D. Dissertation, Department of Mechanical Engineering, University of Minnesota, 2001.

[28] S.M. You, Pool boiling heat transfer with highly-wetting dielectric fluids, Ph.D. Thesis, Department of Mechanical Engineering, University of Minnesota, Minneapolis, 1990.

[29] Sandia, Chip Packages Manual, Sandia National Labs, 1999.

[30] Robert J. Moffat, Describing the uncertainties in experimental results, Exp. Thermal Fluid Sci. (1988) 3–17.

[31] I. Mudawar, A.H. Howard, C. Gersey, An analytical model for near saturated pool boiling critical heat flux on vertical surfaces, Int. J. Heat Mass Transfer (1997) 2327.

[32] M.J. Brusstar, H. Merte, R.B. Keller, B. Kirby, Effects of heater surface orientation on the critical heat flux—I. An experimental evaluation of models for subcooled pool boiling, Int. J. Heat Mass Transfer 40 (17) (1997) 4007–4019.